2.5-μm InGaAs photodiodes grown on GaAs substrates by interfacial misfit array technique

Pamela Jurczak[1], Kimberly A. Sablon[2], Marina Gutiérrez[3], Huiyun Liu[1], and Jiang Wu[1,*]

[1] Department of Electronic and Electrical Engineering, University College London, Torrington Place, London, WC1E 7JE, United Kingdom

[2] United States Army Research Laboratory, 2800 Powder Mill Road, Adelphi, Maryland 20783-1197, United States of America

[3] Department of Material Science and Metallurgic Engineering, The University of Cadiz, 11510, Puerto Real, Cadiz, Spain

*Email: jiang.wu@ucl.ac.uk

Abstract

$In_{0.85}Ga_{0.15}As$ photodetectors grown on GaAs substrates using an interfacial misfit array-based simple buffer are studied. The material quality is assessed with a range of characterization tools showing low surface roughness and low density of threading dislocations. These results indicate a significant improvement on crystal quality compared to structures grown on InP substrates by using metamorphic buffers. Quantum efficiency and responsivity measurements show good performance of the fabricated devices between 1.5 and 2.5 μm, making them highly suitable for short-wavelength infrared applications.

Keywords: infrared; photodiodes; epitaxy; interfacial misfit array; short-wavelength

Introduction

InGaAs short-wavelength infrared (SWIR) detectors are widely used in space remote sensing, environment monitoring, night vision, spectroscopy, etc. [1]. The $In_{0.53}Ga_{0.47}As$ photodetectors lattice-matched to InP substrate have a limited cut-off wavelength of 1.7 μm. Among many of these applications, e.g. gas sensing, it is highly desirable to extend the cut-off wavelength beyond 2.5 μm. To meet such a goal, the indium content in $In_xGa_{1-x}As$ must be increased to 80%~85%, which results in a large lattice mismatch (+1.85% ~ +2.2%) between the InGaAs

layers and the commonly used InP substrates. A number of methods have been adopted to achieve ternary InGaAs with high indium composition on InP substrates, including dilute bismides, e.g. quaternary InGaAsBi[2] and graded InAlAs metamorphic buffers[3,4]. The former has successfully demonstrated InGaAsBi SWIR detectors with the cut-off detection wavelengths up to 2.1 μm, but the difficulty in bismuth incorporation in InGaAs makes it challenging to further extend the detection wavelength. Over the last ten years, most efforts have been devoted to optimizing the InAlAs metamorphic buffer to achieve high indium composition InGaAs on InP substrates. A SWIR detectors made of high indium content $In_xGa_{1-x}As$ (x=90%) have been successfully demonstrated with cut-off wavelengths up to 2.9 μm[5]. However, the large lattice mismatch of more than 2.0% requires a rather thick and complicated buffer structure to accommodate the strain-induced dislocations.

In this paper, we report a simple buffer (less than 1 μm in thickness) using the interfacial misfit array technique to grow extended wavelength InGaAs photodiodes on virtual GaSb/GaAs substrates. The interfacial misfit array technique can effectively relieve the strain caused by the large lattice mismatch (~7.8%) between the intermediate GaSb epilayer and the GaAs substrate[6]. The virtual GaSb/GaAs substrate can then be used to grow $In_xGa_{1-x}As$ (x>85%) with a thin buffer because the lattice mismatch is relatively small (<1.6%). Otherwise, very thick InAlAs metamorphic buffers are required for growing high indium content $In_{0.85}Ga_{0.15}As$ on GaAs substrates (lattice mismatch ~ 6.1%)[7,8]. The use of GaAs substrates also provides a cost effective solution for detector manufacturing due to availability of low cost, high quality, and large-size (up to 6 inch) wafers[6,8]. Additionally, the SWIR detectors grown on a GaAs substrate can also take advantage of the well-established GaAs electronic device technology for monolithically integrated sensors and infrared focal plane arrays[9].

Experimental Details

The InGaAs detector sample and a test GaSb sample have been grown on a highly-p-doped, epi-ready (001) GaAs substrates using a solid source molecular beam epitaxy (MBE) system. For the test sample, a thin GaSb layer was grown directly on the GaAs surface with the interfacial misfit array technique. For the detector sample, several buffer layers have been used to accommodate for the lattice mismatch between GaAs and $In_{0.85}Ga_{0.15}As$. First, a thin GaSb layer was grown using the same conditions as the test sample at ~510 ºC. Sequentially, an InAs buffer layer was grown followed by a graded InAlAs buffer and then InAlAs/InAlGaAs superlattice. The InGaAs and InAlAs layers were grown at ~460 ºC. Beryllium doping has been applied to all of the aforementioned layers, resulting in doping levels of N_a=5×10^{18} cm^{-3}. After all the buffer layers, a 1000-nm-thick, 2.5×10^{18} cm^{-3} doped p-type $In_{0.85}Ga_{0.15}As$ layer has been grown, followed by 500 nm of intrinsic $In_{0.85}Ga_{0.15}As$ and then 250 nm of n-type 1.5×10^{18} cm^{-3} doped $In_{0.85}Ga_{0.15}As$, all together forming the active region of the device. N-type $In_{0.85}Al_{0.15}As$ window layer has been grown on top of it, also with a 1.5×10^{18} cm^{-3} doping level, and finally the contacting $In_{0.85}Ga_{0.15}As$ with a higher doping level of 5×10^{18} cm^{-3}. The full structure of the grown photodiode is shown in Figure 1(a). Photodetectors with different mesa sizes have been processed using the standard photolithography. Ohmic contacts (20 nm/200 nm Ti/Au for both p and n type contacts) on the detector pixels are deposited using e-beam evaporation followed by a liftoff process and then thermal annealing at 420°C for 30 seconds in order to minimise the impact of contacts resistance. Detector responsivity and quantum efficiency spectra are obained in front-illumination configuration by measuring the relative spectral response in a Fourier-transform infrared spectrophotometer. Photocurrent in a narrow spectral band around 2 microns is first measured with a bandpass filter and a calibrated blackbody source at 1000 °C using three different blackbody aperture sizes. The slope of the current versus photon flux from each aperture curve gives the average quantum efficiency at 2 microns. This is then used to scale the relative spectral data to give the quantum efficiency (electrons/photon) and the responsivity (A/W) spectra. A detector used in the measurements has a mesa size about 50 μm in diameter.

Results and Discussion

Figure 1 (b) shows a cross-section SEM image of the entire device, which shows smooth interfaces between the substrate and buffer layers with no obvious structural distortion.

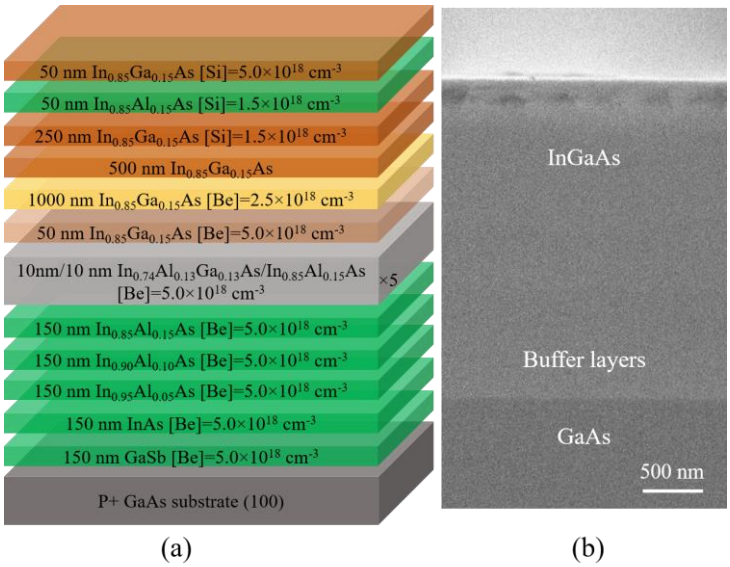

Figure 1. (a) Structure of the $In_{0.85}Ga_{0.15}As$ photodetectors detailing the layers, their thicknesses and compositions. (b) Cross-section SEM micrograph of the In0.85Ga0.15As photodetectors grown on GaAs substrate.

The quality of the grown material has been assessed with scanning electron microscopy (SEM) and transmission electron microscopy (TEM). Looking at the low magnification 220 bright field (BF) TEM micrograph of the whole device structure, from the substrate to the top contacting layer, it can be observed that there are some threading dislocations (TDs) propagating through the upper layers of the cell (Figure 2 (a)). It results in virtually perfect crystal quality in the uppermost layers of the cell, as shown in Figure 2 (b). Figure 2 (c) shows the 220 BF TEM micrographs of the interface substrate-buffer layers where an interfacial misfit dislocation (IMF) network is formed, between the GaAs substrate and GaSb, which effectively relieved the strain caused by the large lattice mismatch (7.8%). The IMF transition layer is thicker than previous reports as a result of the solid solution hardening of the GaSb alloy. In other words, with a high doping concentration at this layer, the glide of the misfit dislocations towards the interface is suppressed [10]. The TDs originating from this IMF are mainly confined in the three bottom buffer layers, GaSb, InAs and InAlAs, as shown in Figure 2(d). So the density of the TDs in the active area of the cell is significantly lower than in the bottom filtering layers giving place to a high quality active region.

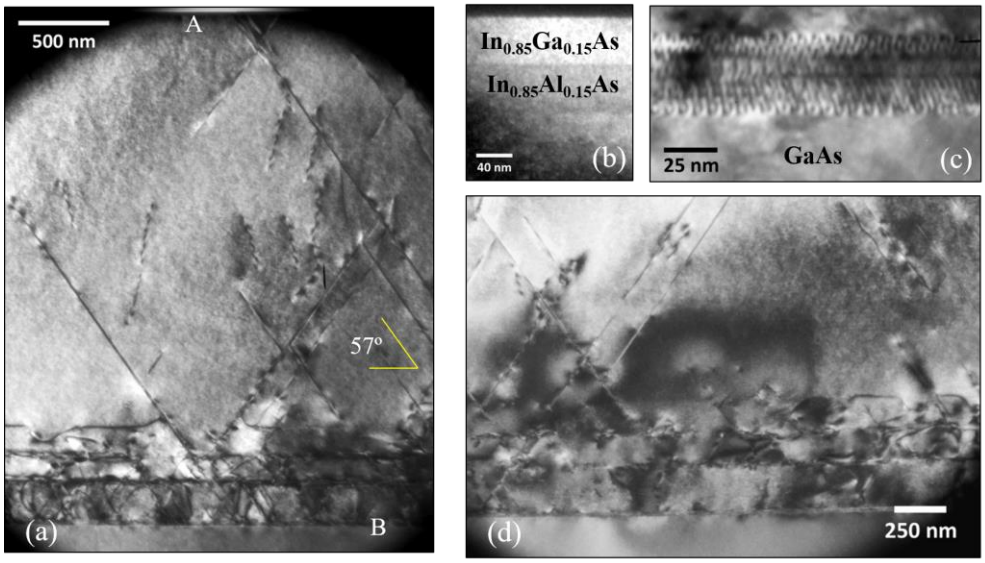

Figure 2. Cross section 220 BF TEM micrographs of the InGaAs photodiode showing different layers within the structure: (a) the entire device structure, (b) the top layers taken from position A in (a), (c) the IMF formed at the GaSb/GaAs interface taken from position B in (a) and (d) the evolution of TDs at the different buffer layers.

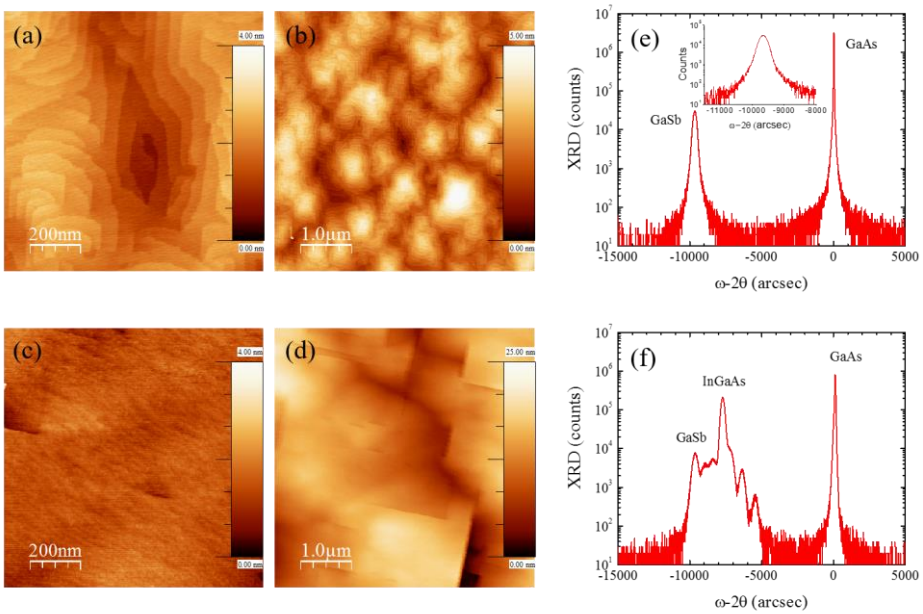

Figure 3. AFM images of (a,b) GaSb intermediate layer and (c,d) InGaAs photodiode grown on GaAs. (a,c) are 1μm × 1μm AFM images with z-scale of 4.0 nm and (b,d) are 5μm × 5μm AFM images with z-scale of 5.0 nm and 25 nm, respectively. XRD curves for (e) GaSb intermediate layer and (f) InGaAs photodiode grown on GaAs. The inset in (e) is the XRD curve of the GaSb layer grown on GaAs.

Figure 3 (a)-(d) shows AFM images of the surfaces of GaSb intermediate layer and the InGaAs photodiode wafer at different scanning scales. As shown in Fig. 3 (a), very smooth surface with clear atomic steps and terraces as wide as 50 nm can be observed. A large-scale AFM image (5μm × 5μm) in Fig. 3 (b) also shows a smooth surface with a low root mean square (RMS) roughness of 0.75 nm. The observation of smooth GaSb surface by AFM

measurements is in good agreement with the low threading dislocation density of the GaSb layer measured by TEM. Figure 3 (c) shows the surface morphology of the InGaAs photodiode. No surface terrace was observed in the 1μm × 1μm AFM image shown in Fig. 3 (c). From the scale bar (z = 4 nm), it can be observed that on micro-scale the roughness of the sample is still low. However, compared with the GaSb surface, the RMS roughness measured from the 5μm × 5μm AFM image of the InGaAs photodiode surface is increased to 4.03 nm. Additionally, surface defects, likely misfit segments, are clearly visible in the AFM images. As shown in the TEM images, most of the dislocations are generated as the lattice is graded from GaSb to $In_{0.85}Ga_{0.15}As$. Compared to metamorphic buffers with lattice grading from InP or GaAs to $In_xGa_{1-x}As$ (x>85%), the current approach can provide a high quality virtual substrate with a smaller lattice mismatch and hence is more favorable.

X-ray diffraction has been used to assess the quality of the grown materials. Figure 3(e) and (f) shows the results of XRD measurements of samples with only a thin GaSb layer and an InGaAs photodiode structure, respectively. As shown in Fig. 3(e), the GaSb layer grown on the GaAs substrate shows a relatively narrow diffraction peak with FWHM of ~280 arcsec which is comparable the state-of-the-art GaSb grown on GaAs substrates[11]. Figure 3(f) shows the XRD curve measured for the InGaAs photodiode. Diffraction peaks from the GaAs substrate, the GaSb buffer and the InGaAs active region are clearly distinguishable. The highest peak corresponds well to a fully relaxed $In_{0.85}Ga_{0.15}As$ layer. Again, a very narrow FWHM (~270 arcsec) is measured from the diffraction peak of the InGaAs layer. The FWHM value measured here is only about half of the reported values from InGaAs layers grown on InP and GaAs substrates using metamorphic buffers[12,13]. Such a low FWHM indicates high quality of the InGaAs layers.

Figure 4 (a) shows the dark current measured from the InGaAs photodiode. Although good structural quality has been confirmed by TEM and XRD measurement, relatively high leakage current has been observed. At negative bias, the dark current only reduced by less than one order of magnitude, indicating that diffusion current and generation-recombination current, which are strongly temperature dependent, are not the major component of the dark current. Therefore, this high dark current could be attributed to large surface leakage as no surface passivation has been applied. With surface passivation, the dark current is expected

to be significantly reduced[14]. Despite a large dark current, a photocurrent has been measured using a calibrated 1000°C blackbody source at room temperature (Fig. 4 (b)). The current vs. voltage (IV) curves in Fig. 4(b) were measured by placing the sample close to the aperture of the 1000 °C blackbody. The aperture was blocked by a shutter over the sample for dark IV measurements. By subtracting the dark current component, the photocurrent density is calculated to be as high as ~500 mA/cm^2. Figure 4 (c) shows the results of quantum efficiency and responsivity measurements for the $In_{0.85}Ga_{0.15}As$ photodiode investigated. The relative spectral response in the Fourier Transform Infrared Spectroscopy (FTIR) and the photocurrent in a narrow spectral band around 2.0 μm have been measured using a calibrated blackbody source at 1000°C with three different aperture sizes. The slope of the current versus photon flux for the different apertures gives the average quantum efficiency at 2 μm. This was used to scale the relative spectral data to obtain the efficiency in electrons per photon and responsivity in amps per watt. As can be seen from the plots in Figure 4 (c), the extended wavelength InGaAs photodiode shows a spectral response with 50% cut-off wavelength up to 2.5 μm. A high responsivity of 0.7 A/W and quantum efficiency of up to 50% were obtained. The highest responsivity and quantum efficiency has been measured at around 2 μm. A clear declining of quantum efficiency from 1.5 to 2.5 μm is observed. As the number of threading dislocations reduces with the epi-layer thickness, the lower active has a high density of threading dislocations and thus reduced carrier diffusion length. As a result, the quantum efficiency at longer wavelength is significantly reduced. All of the quantum efficiency related measurements have been carried out at low temperatures (78 K).

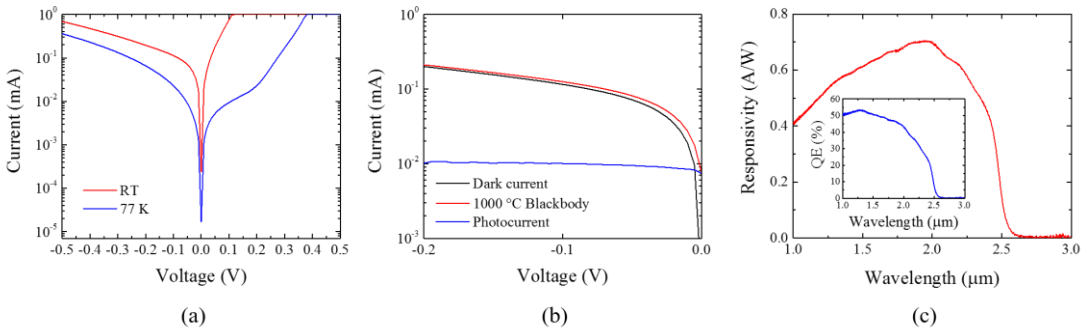

Figure 4. (a) Dark I-V characteristics of the photodiode measured at 77 K and room temperature. (b) Photocurrent measured with a 1000°C blackbody source at room temperature. (c) Responsivity spectrum for the $In_{0.85}Ga_{0.15}As$ cells at 77 K under a 1000°C blackbody source. The inset shows the quantum efficiency spectrum.

Conclusions

We have successfully grown InGaAs photodetectors with indium content of 85% on a GaAs substrate. The interfacial misfit array technique was used to form a high quality GaSb/GaAs virtual substrate to grow $In_{0.85}Ga_{0.15}As$ with less lattice mismatch, compared with InP and GaAs substrates. SEM, TEM and XRD measurements confirmed high quality of the grown material with low surface roughness and threading dislocation density. The QE and responsivity measurements showed that the performance of the devices is good, yielding quantum efficiency of about 50%. High responsivity levels have been measured at around 2 μm with 50% cut-off wavelength up to 2.5 μm. A declining quantum efficiency from 1.5 to 2.5 μm indicates that a relatively high defect density reduces the diffusion length of minority carriers in the p-region of the device. Further optimization of the buffer layers is still required. These results indicate that the structure presented in this paper is a good alternative to the InGaAs photodetector devices grown on InP substrates.

References

[1] RW Hoogeveen, AP Goede. Extended wavelength InGaAs infrared (1.0–2.4 μm) detector arrays on SCIAMACHY for space-based spectrometry of the Earth atmosphere, Infrared Phys.Technol. 42 (2001) 1-16.

[2] Y Gu, Y Zhang, X Chen, Y Ma, S Xi, B Du, et al. Nearly lattice-matched short-wave infrared InGaAsBi detectors on InP, Appl.Phys.Lett. 108 (2016) 032102.

[3] Y Zhang, Y Gu, Z Tian, A Li, X Zhu, K Wang. Wavelength extended InGaAs/InAlAs/InP photodetectors using n-on-p configuration optimized for back illumination, Infrared Phys.Technol. 52 (2009) 52-56.

[4] B Du, Y Gu, Y Zhang, X Chen, S Xi, Y Ma, et al. Effects of continuously or step-continuously graded buffer on the performance of wavelength extended InGaAs photodetectors, J.Cryst.Growth. 440 (2016) 1-5.

[5] C Li, Y Zhang, K Wang, Y Gu, H Li, Y Li. Distinction investigation of InGaAs photodetectors cutoff at 2.9 μm, Infrared Phys.Technol. 53 (2010) 173-176.

[6] KC Nunna, SL Tan, CJ Reyner, ARJ Marshall, B Liang, A Jallipalli, et al. Short-wave infrared GaInAsSb photodiodes grown on GaAs substrate by interfacial misfit array technique, IEEE Photonics Technology Letters. 24 (2012) 218-220.

[7] L Zimmermann, J John, S Degroote, G Borghs, C Van Hoof, S Nemeth. Extended wavelength InGaAs on GaAs using InAlAs buffer for back-side-illuminated short-wave infrared detectors, Appl.Phys.Lett. 82 (2003) 2838-2840.

[8] L Zhou, Y Zhang, X Chen, Y Gu, H Li, Y Cao, et al. Dark current characteristics of GaAs-based 2.6 μm InGaAs photodetectors on different types of InAlAs buffer layers, J.Phys.D. 47 (2014) 085107.

[9] C Xie, V Pusino, A Khalid, MJ Steer, M Sorel, IG Thayne, et al. Monolithic Integration of an Active InSb-Based Mid-Infrared Photopixel with a GaAs MESFET, IEEE Trans.Electron Devices. 62 (2015) 4069-4075.

[10] M. Gutiérrez, O. Bazta, D. Araujo, P. Jurczak, J. Wu and H. Liu, Solid solution strengthening in GaSb/GaAs: A mode to reduce the TD density through Be-doping. Appl. Phys. Lett., 2017.

[11] Z Tian, S Krishna. Mid-infrared metamorphic interband cascade photodetectors on GaAs substrates, Appl.Phys.Lett. 107 (2015) 211114.

[12] X Chen, Y Gu, Y Zhang, S Xi, Z Guo, L Zhou, et al. Optimization of InAlAs buffers for growth of GaAs-based high indium content InGaAs photodetectors, J.Cryst.Growth. 425 (2015) 346-350.

[13] Y Zhang, Y Gu, Z Tian, K Wang, A Li, X Zhu, et al. Performance of gas source MBE-grown wavelength-extended InGaAs photodetectors with different buffer structures, J.Cryst.Growth. 311 (2009) 1881-1884.

[14] Y Zhou, X Ji, M Shi, H Tang, X Shao, X Li, et al. Impact of SiNx passivation on the surface properties of InGaAs photo-detectors, J.Appl.Phys. 118 (2015) 034507.